INTERNATIONAL JOURNAL OF PRECISION ENGINEERING AND MANUFACTURING Vol. 19, No. 8, pp. 1171-1177 AUGUST 2018 / 1171

REGULAR PAPER

DOI: 10.1007/s12541-018-0138-4
ISSN 2234-7593 (Print) / 2005-4602 (Online)

# Three-Dimensional Numerical Analysis of Weld Pool in GMAW with Fillet Joint

**Hunchul Jeong[1], Kyungbae Park[1], Sungjin Baek[1], Dong-Yoon Kim[2], Moon-Jin Kang[2], and Jungho Cho[1,#]**

1 School of Mechanical Engineering, Chungbuk National University, 1, Chungdae-ro, Seowon-gu, Cheongju-si, Chungcheongbuk-do, 28644, Republic of Korea
2 Joining R&D Group, Korea Institute of Industrial Technology, 156, Gaetbeol-ro, Yeonsu-gu, Incheon, 21999, Republic of Korea
# Corresponding Author / E-mail: junghocho@cbnu.ac.kr, TEL: +82-43-261-2445
ORCID: 0000-0003-2165-2692

KEYWORDS: Weld pool, CFD, GMAW, Volume of fluid, Steel, Automotive

*GMA welding is widely used in many different fields such as automotive, shipbuilding and plant industry and its demand is growing day by day because of its high productivity and quality with cost reduction in manufacturing process. Nevertheless, the studies have been reported just a few cases so far due to its difficulties in expressions for the complexity of physical phenomena and in the derivation of the mathematical models. In this research, its complex numerical models including three-dimensional heat flux, arc pressure and electromagnetic force are newly suggested and its validation is proved through the comparison between the experimental and simulation results. Basically, the arc heat flux, arc pressure and Marangoni flow are employed as the boundary conditions. And electromagnetic force and buoyancy are realized as body terms. The governing equations such as the continuity, momentum, VOF and energy equations are adopted as usual simulations. It is, however, that only these equations cannot fulfill all requirements to investigate the behavior of the weld pool in GMA welding. To compensate the insufficient, three-dimensional mathematical model and coordinate transform of arc are newly suggested to reflect the twisted torch angle and arc effective radius change according to the distance from electrode tip. Suggested analysis model is verified through comparison to lap joint fillet GMAW experiment of steel sheets for automotive industry and it shows successful correspondence.*

Manuscript received: March 13, 2018 / Revised: May 4, 2018 / Accepted: May 15, 2018

## NOMENCLATURE

B = magnetic flux density
$C_A$ = concentration coefficent of arc
$C_p$ = specific heat at constant pressure
F = volume fraction occupied by fluid
$F_x$ = force in the x direction
$F_y$ = force in the y direction
$F_z$ = force in the z direction
$g_z$ = gravitational acceleration in the z direction
$h$ = enthalpy
$h_A$ = convection coefficient
I = welding current
$J$ = current density
$J_z$ = current density in the z dirction
K = thermal conductivity
$L_f$ = latent heat of fusion
n = normal component
P = pressure
$P_A$ = arc pressure
$q_A$ = heat input by arc
$q_d$ = heat input by droplet
$r_A$ = effective radius of arc
$r_d$ = droplet radius
$R_x$ = coordinate transformation matrix for x axis
$R_y$ = coordinate transformation matrix for y axis
T = temperature
$T_d$ = droplet temperature
t = time
$T_l$ = liquidus temperature
$T_s$ = solidus temperature
$T_\infty$ = ambient temperature
V = welding voltage

$\vec{V}$ = velocity vector
x, y, z = coordinate index in local coordinate system
x', y', z' = coordinate index in global coordinate system

**Greek symbols**

$\beta$ = volume thermal expansion coefficient
$\gamma$ = surface tension
$\varepsilon_s$ =emissivity
$\eta_A$ = heat input efficiency by arc
$\eta_d$ = heat input efficiency by droplet transfer
$\theta$ = travel angle for torch
$\mu$ = viscosity
$\mu_m$ = magnetic permeability of metal
$\mu_0$ = magnetic permeability in vaccum
ν = dynamic viscosity
π = circular constant
$\rho$ = density
$\sigma$ = normal stress
$\sigma_s$ = Stefan-Boltzmann constant
$\tau$ = shear stress,surface tangential direction
$\phi$ =work angle for torch

## 1. Introduction

Among many welding processes, GMAW (gas metal arc welding) is one of the most widely used welding processes in automotive, plant and shipbuilding industries owing to its higher productivity than that of other welding processes. It is, however, limited to freely control welding parameters and welding conditions to assure weld good quality due to the complexity of the physical phenomena. Simulations through numerical methods have been sometimes employed to understand physical phenomena of GMAW and help adjusting process variables.[1] Most of numerical studies of weld pool in GMA welding mainly focused on the welding on the bead-on-plate (BOP) with electrode's vertical position and its formulations are basically composed of two-dimensional mathematical equations regarding heat flux and arc pressure models applied on top surface.[9] The majority of the GMA welding has a fillet[12-15] or lap joint type laid in inclined torch position instead of its vertical position which is commonly used on BOP welding. Wu et al.[2] presented the mathematical model considering tilted torch position by using the coordinate rotation however it dealt only work angle.

In this research, three-dimensional mathematical heat flux and arc pressure models are newly suggested considering the arc effective radius varied with the distance from electrode tip. In addition, it is considering torch posture of not only work angle but also travel angle as seen in Figs. 1 and 2.

The numerical analysis model is assumed to be incompressible, Newtonian fluid and laminar flow. Governing equations consist of the continuity equation, Navier-Stokes equation and energy equation. In addition to these three basic equations, conservative governing equation

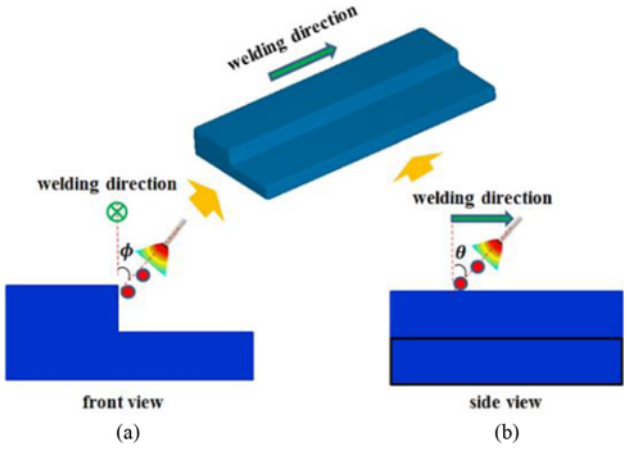


Fig. 1 Definition of the torch posture; (a) work angle, (b) travel angle

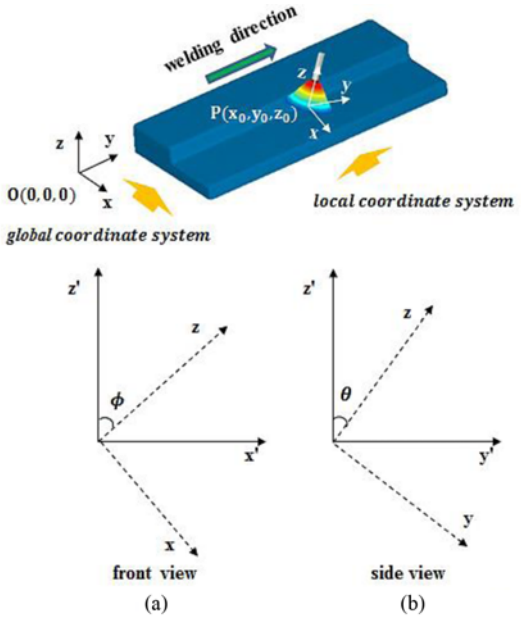


Fig. 2 Concept of coordinate transformation; (a) work angle, (b) travel angle

of fluid fraction is accompanied to track the free surface of fluid which is well known technique as VOF (volume of fluid) method. With these four governing equations, several numerical boundary conditions are included to the simulation such as arc heat flux, arc pressure and surface tension gradient by temperature of the molten pool. The molten pool analysis model also includes electromagnetic force and buoyancy as body force term in Navier-Stokes equation. This basic model already has been verified through the authors' previous reports.[3-6]

## 2. Mathematical Model

### 2.1 Coordinate transformation

Welding characteristic equations including arc heat flux, arc pressure and electromagnetic force to determine the behavior of the weld pool can be simply derived and expressed in BOP welding with perpendicular

torch because global coordinate and torch's local coordinate have only linear translation relationship, however, the equations become complex if the torch has twisted posture in fillet welding like Fig. 2. This kind of complex torch posture is unusual because most of cases the torch has only work angle. In this research, zinc coated steel sheets are GMA welded and various torch postures are tried to reduce the zinc porosity therefore the torch has travel angle either.

Conventional arc heat flux and electromagnetic force model needs to be converted with respect to the relationship between global coordinate and torch's local coordinate system. Because arc heat flux has eccentric ellipsoidal distribution rather than Gaussian if the torch is tilted for example. Fig. 2 shows the general concept to indicate the coordinate transformations composed of two welding angles. Where $\theta$ and $\phi$ indicate the travel angle and work angle, respectively as aforementioned. Numerical expression for coordinate rotation by each angle is followed as the coordinate transformation matrices, $R_{x(\theta)}$ and $R_{y(\phi)}$.

$$R_{x(\theta)} = \begin{bmatrix} 1 & 0 & 0 \\ 0 & \cos\theta & \sin\theta \\ 0 & -\sin\theta & \cos\theta \end{bmatrix}$$
$$R_{y(\phi)} = \begin{bmatrix} \cos\phi & 0 & -\sin\phi \\ 0 & 1 & 0 \\ \sin\phi & 0 & \cos\phi \end{bmatrix} \quad (1)$$

Accordingly, the converted global coordinate system, $(x', y', z')$ could be expressed as follows.

$$\begin{bmatrix} x' \\ y' \\ z' \end{bmatrix} = R_{x(\theta)} R_{y(\phi)} \begin{bmatrix} x \\ y \\ z \end{bmatrix} \quad (2)$$

If the equation on a basis of the global coordinate system is converted into that of the local coordinate including linear translation, it becomes as following Eq. (3).

$$\begin{bmatrix} x \\ y \\ z \end{bmatrix} = \begin{bmatrix} \cos\phi & \sin\theta\sin\phi & \cos\theta\sin\phi \\ 0 & \cos\theta & -\sin\theta \\ -\sin\phi & \sin\theta\cos\phi & \cos\theta\cos\phi \end{bmatrix} \begin{bmatrix} x'-x_0 \\ y'-y_0 \\ z'-z_0 \end{bmatrix} \quad (3)$$

Where, $x_0$, $y_0$ and $z_0$ denote the position of the electrode tip away from the global coordinate system's origin. Eq. (3) offers a hint to be compatible with the any kind of physical values in local and global coordinate system through its transformation.

### 2.2 Governing equations

In present work, four basic governing equations are employed as usual simulation of GMAW molten pool. The first one is the VOF (volume of fluid) method which is based on variable F. Its value depends on volume fraction of fluid occupying in each cell. By definition, the value of F is defined as 0 in void cell, 1 in fully occupied cell and otherwise, a value between 0 and 1, which is recognized as free surface elements as seen in Fig. 3. Conservation of F is expressed as following Eq. (4).[7]

$$\frac{DF}{Dt} = \frac{\partial F}{\partial t} + \nabla \cdot (\vec{V}F) = 0 \quad (4)$$

As aforementioned, the fluid for this analysis is regarded as incompressible. By the assumptions, the continuity equation is expressed as follows.


Fig. 3 A schematic diagram of expressing volume fraction

$$\nabla \cdot \vec{V} = 0 \quad (5)$$

With the above assumptions, the fluid is dealt with Newtonian. The conservation equation of the momentum is also induced as following Navier-Stokes Eq. (6).[8]

$$\frac{DV}{Dt} = -\frac{1}{\rho}\nabla P + \nu\nabla^2 V + g_z[1-\beta(T-T_m)] \quad (6)$$

Where, the buoyancy force is added to the gravitational force in the last term on the right-hand side of Eq. (6) with an assumption that the volume change by temperature is small enough to be negligible based on the Boussinesq approximation for natural convection.

The arc heat input is intensively imposed as heat flux boundary condition on the free surface near the region in which the arc is positioned. Then, the heat is transferred into base metal by means of direct heat transfer method such as conduction and convection throughout the weld pool. The energy equation is only considering conservation of thermal energy in weld pool. Hence the kinetic and potential energies in the molten pool are assumed to be negligible comparatively. Latent heat of fusion in the enthalpy term of energy conservation equation is divided into three different cases by phase conditions. By taking all these considerations into account, the conservation of energy is expressed as follows.

$$\frac{dh}{dt} + (\vec{V}\cdot\nabla)h = \frac{1}{\rho}\nabla\cdot(K\nabla T) \quad (7)$$
$$h = C_p \cdot T + f(T)\cdot L_f \quad (8)$$
$$f(T) = \begin{cases} 0, & T \le T_s \\ \dfrac{T-T_l}{T_l-T_s}, & if\ T_s < T < T_l \\ 1, & T \ge T_l \end{cases} \quad (9)$$

Where, the last term of the right-hand side in Eq. (8) represents the latent heat of fusion during melting. Consequently, it depends on the volume fraction of liquid phase $f_{(T)}$.

### 2.3 Arc welding characteristics

#### 2.3.1 Three dimensional mathematical models

Numerical models for heat flux and arc pressure added on top surface while welding is assumed to be the Gaussian distribution. In the past, all of them were dealt with two-dimensional planar mathematical model. It means that the arc effective radius would be assumed to be constant on a plane regardless the distance between the plane and arc, i.e., arc length. However, it could be easily supposed that arc effective radius is varied with the arc length. The present work considers three-dimensional numerical model and formulates it with an assumption that arc effective radius, $r_A$, is linearly affected by arc length. Fig. 4 is a graph

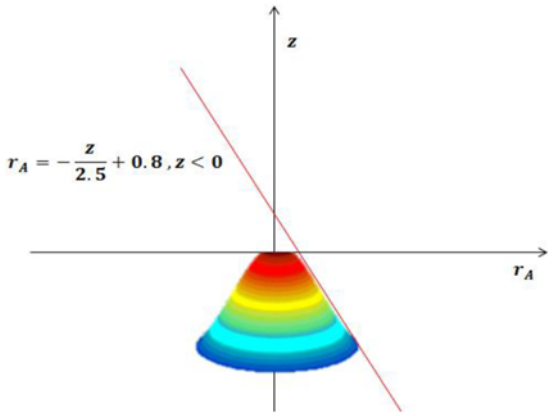


Fig. 4 A correlation between art effective radius and the distance away from arc source (unit: mm)

showing its correlation and its mathematical model is expressed as follows.

$$r_A = -\frac{z}{2.5} + 0.8, \quad z < 0 \tag{10}$$

Where, the unit length used in its formulation is 'mm'. Accordingly, 3-D numerical arc heat flux, arc pressure and electromagnetic force models could be derived as following equations.

$$q_A(x,y,z) = \eta_A \frac{VI}{2\pi r_A^2} \exp\left\{-\frac{x^2+y^2}{2r_A^2}\right\} \tag{11}$$

$$\begin{aligned} P_A(x) &= \frac{\mu_0 I^2}{4\pi^2 r_A^2} \exp\left(\frac{x^2+y^2}{2r_A^2}\right) \sin\phi \hat{i}' \\ P_A(y) &= -\frac{\mu_0 I^2}{4\pi^2 r_A^2} \exp\left(\frac{x^2+y^2}{2r_A^2}\right) \sin\theta\cos\phi \hat{j}' \\ P_A(z) &= -\frac{\mu_0 I^2}{4\pi^2 r_A^2} \exp\left(\frac{x^2+y^2}{2r_A^2}\right) \cos\theta\cos\phi \hat{k}' \end{aligned} \tag{12}$$

Eqs. (11) and (12) indicate the three dimensional arc heat flux and arc pressure model, respectively. As the arc pressure is always forced in the parallel direction to the axis of electrode, i.e., there is only z-axis component vector in local coordinate system, it should be converted into the unit vector components ($\hat{i}'$, $\hat{j}'$, $\hat{k}'$) in global coordinate system.

Electromagnetic force while welding plays a role as body force in control volume for welding simulation. Basically, the Lorentz force is cross product of current density J and magnetic field B as[10]

$$F = J \times B \tag{13}$$

When electrons are transmitted from cathode to anode, they are always emitted or absorbed in normal direction, i.e., current density is only normal to anode or cathode surface. However, the weld pool surface always changes therefore it becomes extremely complex problem if the electromagnetic force should be derived along the free surface at every single moment. Therefore a previous research about electromagnetic force model in arc welding made the solution simple with flat surface. Detailed descriptions for the assumptions would become as follows.

1) Electrical conductivity and magnetic permeability were considered as only constant.

$$\frac{\partial K}{\partial T} = \frac{\partial \mu_m}{\partial T} = 0$$

2) Current flux density is according to the Gaussian distribution as

$$J_z = \frac{I}{2\pi r_A^2} \exp\left(-\frac{r^2}{2r_A^2}\right)$$

3) Magnetic flux density in the radius direction and normal direction in cylindrical coordinator system is assumed to be zero.

4) The current flux density in the radius direction would be averagely equal throughout whole thickness for the base metal.

Based on a former research[10] for electromagnetic force in welding process, following Eq. (14) can be derived by reflecting the coordinate and vector transformation to fit well in GMA welding.

$$\begin{aligned} F_x &= -\frac{I^2\mu_m}{4\pi^2 r r_A^2} \exp\left(-\frac{r^2}{2r_A^2}\right)\left\{1-\exp\left(-\frac{r^2}{2r_A^2}\right)\right\}\left(1-\frac{z}{c}\right)^2 \frac{x}{r}\cos\phi \\ &\quad -\frac{I^2\mu_m}{4\pi^2 r^2 c}\left\{1-\exp\left(-\frac{r^2}{2r_A^2}\right)\right\}^2\left(1-\frac{z}{c}\right)\sin\phi \\ F_y &= -\frac{I^2\mu_m}{4\pi^2 r r_A^2} \exp\left(-\frac{r^2}{2r_A^2}\right)\left\{1-\exp\left(-\frac{r^2}{2r_A^2}\right)\right\}\left(1-\frac{z}{c}\right)^2 \frac{x}{r}\sin\theta\sin\phi \\ &\quad -\frac{I^2\mu_m}{4\pi^2 r r_A^2} \exp\left(-\frac{r^2}{2r_A^2}\right)\left\{1-\exp\left(-\frac{r^2}{2r_A^2}\right)\right\}\left(1-\frac{z}{c}\right)^2 \frac{y}{r}\cos\theta \\ &\quad +\frac{I^2\mu_m}{4\pi^2 r^2 c}\left\{1-\exp\left(-\frac{r^2}{2r_A^2}\right)\right\}^2\left(1-\frac{z}{c}\right)\sin\theta\cos\phi \\ F_z &= -\frac{I^2\mu_m}{4\pi^2 r r_A^2} \exp\left(-\frac{r^2}{2r_A^2}\right)\left\{1-\exp\left(-\frac{r^2}{2r_A^2}\right)\right\}\left(1-\frac{z}{c}\right)^2 \frac{x}{r}\cos\theta\sin\phi \\ &\quad +\frac{I^2\mu_m}{4\pi^2 r r_A^2} \exp\left(-\frac{r^2}{2r_A^2}\right)\left\{1-\exp\left(-\frac{r^2}{2r_A^2}\right)\right\}\left(1-\frac{z}{c}\right)^2 \frac{y}{r}\sin\theta \\ &\quad +\frac{I^2\mu_m}{4\pi^2 r^2 c}\left\{1-\exp\left(-\frac{r^2}{2r_A^2}\right)\right\}^2\left(1-\frac{z}{c}\right)\cos\theta\cos\phi \end{aligned} \tag{14}$$

### 2.3.2 Pressure boundary condition

In arc welding, the molten surface experiences two kind of pressure boundary condition. One is arc pressure by arc plasma flow[9] and the other is pressure by surface tension. Its mathematical expression for this boundary condition on the top surface can be expressed as follows.

$$-P + 2\mu\frac{\partial V_n}{\partial n} = -P_A + \frac{\gamma}{R_C} \tag{15}$$

Eq. (15) describes boundary condition for pressure on top surface near the weld pool and n denotes the normal direction component. The second term on the left-hand side in Eq. (15) means the shear stress on the weld pool as Newton's viscosity law. In the same equation, second term on the right-hand side describes the pressure by surface tension γ so Rc denotes local surface curvature and the first term on the right-hand side is arc pressure and it is described in Eq. (12).

One of the most interesting features in arc weld pool simulation is

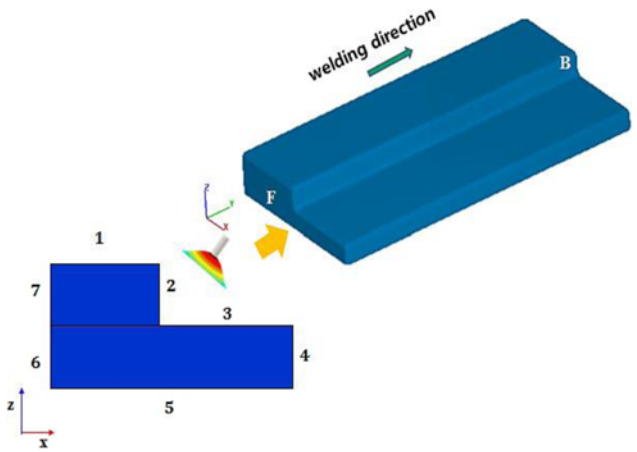


Fig. 5 Schematic diagram of numbering on each boundary surface

Table 1 Boundary conditions on each surface with fillet joint

| Surface No. | 1 | 2 | 3 | 4 | 5 | 6 | 7 | F | B |
|---|---|---|---|---|---|---|---|---|---|
| Boundary condition | A V R | A V R | A V R | C | C | C | C | C | C |

A: arc heat flux / V: convection / R: radiation / C: continuative

that the metal surface is locally melted and its surface tension gradient by temperatures induces shear flow on the molten pool surface. This phenomena is referred to as Marangoni flow and following Eq. (16) is describing its boundary condition. Subscript τ denotes the tangential component.

$$\mu\frac{\partial V_\tau}{\partial n}=\frac{\partial\gamma}{\partial T}\frac{\partial T}{\partial\tau} \tag{16}$$

### 2.3.3 Heat flux boundary conditions

Top surface is the region where the heat flux is activated through arc heat input, convection and radiation emitted by the temperature itself. The other surfaces are imposed natural convection and radiation heat loss except for continuative surface. These are described in Fig. 5 and Table 1.

Among the boundary conditions, C in Table 1 represents the continuative boundary condition as follows.

$$\frac{\partial\Phi}{\partial n}=0 \tag{17}$$

Where, Φ means any kind of physical properties and n denotes the normal direction component of the plane, which means gradient of any kind of thermophysical properties at the plane is zero, accordingly.

Basically evaporational heat loss on the surface near the arc should be considered however it is assumed to be negligible because the arc welding has little influence on evaporation comparing to high power density process such as the laser beam, plasma and electron beam welding. Therefore the boundary condition of top surface is expressed as.

$$K\frac{\partial T}{\partial n}=q_A-h_A(T-T_\infty)-\sigma_s\varepsilon_r(T^4-T_\infty^4) \tag{18}$$

Table 2 Thermophysical properties of the DP590, GA

| Property | Value | Symbol |
|---|---|---|
| Density | S: 6900 / L: 7800 kg/m$^3$ | $\rho$ |
| Thermal conductivity | S: 34.6 / L: 70.0 J·m$^{-1}$·s$^{-1}$·°K | K |
| Specific heat | 620 J·k$^{-1}$·°K | c |
| Solidus temp. | 1713 °K | $T_s$ |
| Liquidus temp. | 1803 °K | $T_l$ |
| Surface tension gradient | -0.2×10$^{-3}$ Nm$^{-1}$°C$^{-1}$ | $\partial\gamma_s$ / $\partial T$ |
| Magnetic permeability | 1.26×10$^{-6}$ H/m | $\mu_m$ |
| Ambient temperature | 298 K | $T_\infty$ |
| Latent heat fusion | 277 kJ/kg | $L_f$ |
| Emissivity | 0.8 | $\varepsilon_r$ |
| Surface tension | 1.2 N·m$^{-1}$ | $\gamma_s$ |
| Convection coefficient | 80 J·m$^{-1}$·s$^{-1}$·°K | $h_A$ |
| Viscosity | 0.006 N·s·m$^{-2}$ | $\mu$ |

S: solid, L: liquid

Table 3 Arc welding parameters and related constants

| Property | Value |
|---|---|
| Welding current | 253 A |
| Welding voltage | 23.5 V |
| Travel speed, $\upsilon_w$ | 0.8 m/min |
| Wire feeding rate | 8 m/min |
| Effective arc radius, $r_A$ | various |
| Thermal efficiency, $\eta_A$ | 0.8 |
| Wire diameter | 1.2 mm |
| Droplet diameter | 1.2 mm |
| Material thickness | 2.6 mm |
| Work angle | -45° |
| Travel angle | 5° |
| Virtual arc length | 3 mm |

In the above Eq. (18), second and third terms on the right side includes are convectional and radiational heat losses respectively.

### 2.3.4 Droplet model

Dhingra et al.[11] stated that total heat input efficiency of GMAW including droplet transfer is from 0.60 to 0.85 therefore it is assumed as 0.8 in this research. The heat amount per a droplet and transfer frequency become as follows.

$$q_d=\frac{4}{3}\pi r_d^3\rho C_p T_d f_d \tag{19}$$

$$f_d=\frac{3r_w^2 V_w}{4r_d^3} \tag{20}$$

Where $T_d$, $r_w$, $r_d$, $f_d$, $V_w$, $\rho$ and $C_P$ represent droplet temperature, wire radius, droplet radius, droplet transfer-frequency, wire feeding speed, density and specific heat respectively. It is noticeable that the droplet is directly transferred to molten pool as realistic volume heat source with the help of VOF method.

## 3. Experiment and Simulation

Material applied in this research is zinc coated DP590 steel sheet which is widely used in automotive industry. The material's

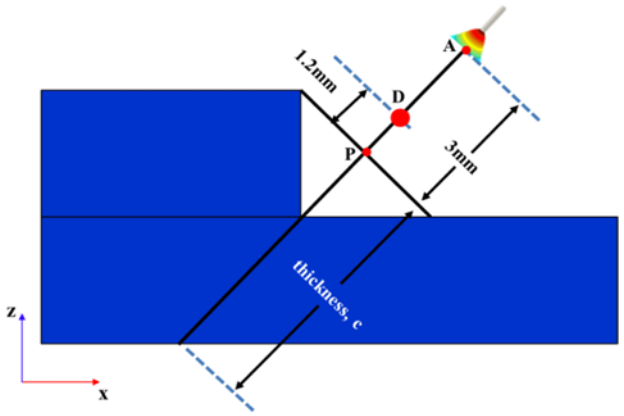


Fig. 6 Determination of the thickness, c, droplet position, D and arc source position, A for simulation

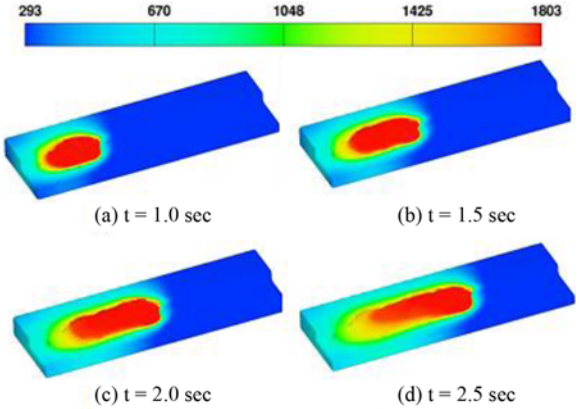


Fig. 7 Three dimensional simulation results by welding time

thermophysical properties and welding process variables are summarized in Table 2 and 3.

Three-dimensional analytic domain is 2.0 cm, 6.4 cm and 1.0 cm in x, y and z direction respectively. Meshed cubic cells have 0.4 mm length in each direction therefore there are totally 200,000 cells. The simulation is conducted by commercial CFD package, Flow-3D. It provides basic solver for free surface tracking, continuity, momentum and energy equations. The other characteristic equations such as electromagnetic force, arc pressure, arc heat flux are formulated in user subroutines. Several assumptions are required to effectively conduct the simulation. Virtual thickness c for electromagnetic force computation, droplet initial position D and electrode position A are set up as Fig. 6. Droplet position is assumed to be fixed at the point D with its velocity, 0.5 m/s.

## 4. Results and Discussions

Representative time sequencial screenshots of three dimensional simulation results are shown in the Fig. 7. Transient molten pool evolution and temperature profile are observed through the images. The length and width of the molten pool can be measured indirectly, whereas it is possible only through high-speed cameras and optical filters in the experiment. Re-solidified weld bead is also seen at the tail

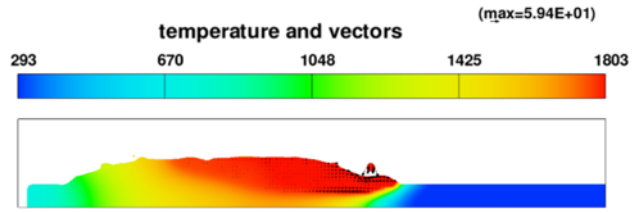


Fig. 8 A representative longitudinal cross sectional screenshot at 2.5 sec after welding

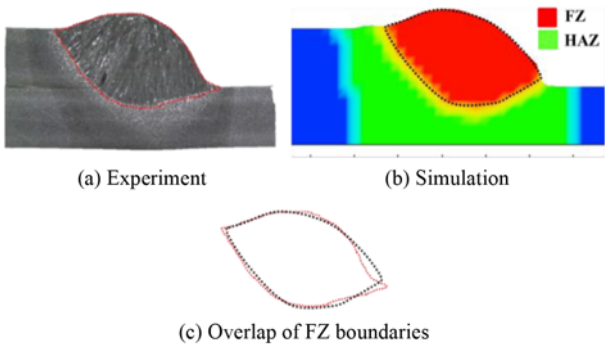


Fig. 9 The comparison between experimental and simulation results in aspect of the FZ boundary in transverse cross section; (a) experiment, (b) simulation, (c) overlap of FZ boundaries between two results

of molten pool. Fig. 8 is longitudinal cross section of the molten pool at 2.5 sec. A droplet is shown at the front part of molten pool. The moment is middle of droplet transfer to molten pool therefore the downward vectors are also shown. The free surface of molten pool in this region has sunken shape due to the strong arc pressure. However it is quickly recovered right behind the region. Re-solidification occurs from lower part of molten pool and it means the hot molten flow is always occupying top area due to buoyancy. Of course the driving force of solidification is conduction heat loss from molten pool to base metal.

General purpose of numerical analysis of manufacturing process is to use it as prediction tool, therefore the main objective of this work is validation of the molten pool analysis model by comparing to experiment. The basic weld bead analysis method is examination of transverse cross section, thus the cross section of simulation is compared to experiment at the same way to examine how accurate the simulation through newly employed mathematical models can be described. Fig. 9 shows the comparison result. Historical temperature profile is achieved through the simulation then FZ (fusion zone) and HAZ (heat affected zone) boundaries are determined on a transverse cross sectional plane which is close to weld end to guarantee fully developed molten pool. As seen in the figure, FZ and HAZ boundaries of simulation are comparatively well coincide with experimental ones. However, there is slight difference at the toe part because of contact angle inaccuracy. It needs to notice that the theoretical contact angle of molten metal is a function of temperature but it is dealt as constant in current work. Furthermore, the information of the contact angle for DP590 was not deeply investigated yet and hence it was set up with 90° in this paper. Although there is minor difference in toe, the accuracy of simulation model is acceptable

because the actual toe angle has insignificant difference according to cross section location. The difference shown in toe angle is just due to the insufficient information about temperature dependent contact angle, therefore this minor difference can be corrected in the future if the contact angle is applied as a function of temperature.

## 5. Conclusions

Although the actual process is applied to butt or lap joint with tilted arc torch, most previous numerical studies of arc weld pool simulation are mainly limited to BOP because they focused on fundamental research to develop accurate analysis model. In this paper, the actual GMAW process of DP590 steel sheet lap joint fillet welding is recreated through three-dimensional numerical analysis. The material and joint type are widely used in subframe members for automotive industry. The arc characteristic equations such as heat input, arc pressure and electromagnetic force are newly adapted to simulation with coordinate transformation according to work and travel angle of tilted torch. Three dimensional effective radius of arc is also newly defined for efficient application of arc heat flux on the lap joint fillet surface. With these special considerations, the distinguished research outputs are summarized as

1) Unlike existing three-dimensional numerical models, work and travel angle of tilted torch are considered and it is confirmed that it can be furthermore generalized in GMA welding simulation.

2) By newly applying the three dimensional arc effective radius varying by the arc length to the three-dimensional numerical analysis in this study, its resultant outputs are valid to effectively describe the FZ, HAZ and bead shape when comparing the experiment.

3) As a result of reviewing simulation through the newly suggested numerical models, backward and upward vortex flow induced by droplet momentum and buoyancy is found in molten pool, which makes the molten flow on top surface remain longer and the bead shape convex.

## ACKNOWLEDGEMENT

This research was supported by Basic Science Research Program through the National Research Foundation of Korea (NRF) funded by the Ministry of Science, ICT and Future Planning, Korea (Grant No. 2016R1D1A1B03935036) and Technology Innovation Industrial Program funded by the Ministry of Trade, Industry & Energy, Korea (Grant No. 10052793 and Grant No. 10077517).

## REFERENCES

1. Rao, Z., Zhou, J., Liao, S., and Tsai, H.-L., "Three-Dimensional Modeling of Transport Phenomena and their Effect on the Formation of Ripples in Gas Metal Arc Welding," Journal of Applied Physics, Vol. 107, No. 5, Paper No. 054905, 2010.
2. Wu, L., Cheon, J., Kiran, D. V., and Na, S.-J., "CFD Simulations of GMA Welding of Horizontal Fillet Joints Based on Coordinate Rotation of Arc Models," Journal of Materials Processing Technology, Vol. 231, pp. 221-238, 2016.
3. Cho, J., "An Analysis of Three-Dimensional Molten Pool in Laser-GMA Hybrid Welding," Ph.D. Thesis, KAIST, 2007.
4. Cho, J.-H., Farson, D. F., Milewski, J. O., and Hollis, K. J., "Weld Pool Flows during Initial Stages of Keyhole Formation in Laser Welding," Journal of Physics D: Applied Physics, Vol. 42, No. 17, Paper No. 175502, 2009.
5. Jeong, H., Park, K., and Cho, J., "Numerical Analysis of Variable Polarity Arc Weld Pool," Journal of Mechanical Science and Technology, Vol. 30, No. 9, pp. 4307-4313, 2016.
6. Jeong, H., Park, K., Kim, Y., Kim, D.-Y., Kang, M.-J., and Cho, J., "Numerical Analysis of Weld Pool for Galvanized Steel with Lap Joint in GTAW," Journal of Mechanical Science and Technology, Vol. 31, No. 6, pp. 2975-2983, 2017.
7. Hirt, C. W. and Nichols, B. D., "Volume of Fluid (VOF) Method for the Dynamics of Free Boundaries," Journal of Computational Physics, Vol. 39, No. 1, pp. 201-225, 1981.
8. Fox, R. W., McDonald, A. T., and Pritchard, P. J., "Introduction to Fluid Mechanics," John Wiley & Sons, 4th Ed., 1992.
9. Cao, Z., Yang, Z., and Chen, X., "Three-Dimensional Simulation of Transient GMA Weld Pool with Free Surface," Welding Journal-New York-, Vol. 83, pp. 169-S-176-S, 2004.
10. Kumar, A. and DebRoy, T., "Calculation of Three-Dimensional Electromagnetic Force Field during Arc Welding," Journal of Applied Physics, Vol. 94, No. 2, pp. 1267-1277, 2003.
11. Dhingra, A. and Murphy, C., "Numerical Simulation of Welding-Induced Distortion in Thin-Walled Structures," Science and Technology of Welding and Joining, Vol. 10, No. 5, pp. 528-536, 2005.
12. Cho, S.-H. and Kim, J.-W., "Thermal Analysis of Horizontal Fillet Joints by Considering Bead Shape in Gas Metal Arc Welding," Science and Technology of Welding and Joining, Vol. 6, No. 4, pp. 220-224, 2001.
13. Kim, C.-H., Zhang, W., and DebRoy, T., "Modeling of Temperature Field and Solidified Surface Profile during Gas-Metal Arc Fillet Welding," Journal of Applied Physics, Vol. 94, No. 4, pp. 2667-2679, 2003.
14. Zhang, W., Kim, C.-H., and DebRoy, T., "Heat and Fluid Flow in Complex Joints during Gas Metal Arc Welding - Part I: Numerical Model of Fillet Welding," Journal of Applied Physics, Vol. 95, No. 9, pp. 5210-5219, 2004.
15. Zhang, W., Kim C-H., and DebRoy T., "Heat and Fluid Flow in Complex Joints during Gas Metal Arc Welding - Part II: Application to Fillet Welding of Mild Steel," Journal of Applied Physics, Vol. 95, No. 9, pp. 5220-5229, 2004.